Available online at www.sciencedirect.com
ScienceDirect
Vision Research 48 (2008) 264–272
Vision Research
www.elsevier.com/locate/visres

Mouse cone photoresponses obtained with electroretinogram from the isolated retina

H. Heikkinen *, S. Nymark, A. Koskelainen

Laboratory of Biomedical Engineering, Helsinki University of Technology, FI-02015 HUT, Finland

Received 3 September 2007; received in revised form 9 November 2007

Abstract

We characterize the dark-adapted photoresponses from mouse cones intact in the isolated retina, their virtually natural environment, by isolating pharmacologically the photoreceptor light responses from the electroretinogram (ERG). Due to the different photoresponse kinetics and sensitivity of rods and cones, the cone responses were readily attained by using a rod-saturating preflash. The stimulus wavelength (544 nm) was chosen to selectively stimulate the green sensitive (''M''-)pigment. Obtained responses were monophasic, showing fast kinetics (mean $t_p = 51$ ms) and low sensitivity (fractional single-photon response ca. 0.23%). The amplification coefficient of cones (4.6 s^{-2}) was very close to that of rods (5.6 s^{-2}), while the dominant time constant of recovery was clearly smaller for cones (33 ms) than for rods (160 ms).

Keywords: Photoreceptor; Retina; Cone; Mouse; Mammal

1. Introduction

Mouse cone photoreceptors are becoming the primary model for studying mammalian cone phototransduction and molecular mechanisms of disease, largely due to the genetic amenability of mouse. However, characterization of the electrical responses of mouse cones to light has been lacking almost completely until very recently, in spite of the emerging importance of the mouse model.

In previous studies the mouse cone function has been investigated with electroretinogram (ERG) flash responses and flicker photometry from live animals, as well as behavioral testing (cf. Lyubarsky, Falsini, Pennesi, Valentini, & Pugh, 1999 and Jacobs, Williams, & Fenwick, 2004). The ERG signal, however, is a complicated signal consisting of several temporally overlapping components, and therefore only the rising phase of the ERG can be attributed to the photoreceptor activity (see for example Hood & Birch, 1990). A further difficulty in assessing the cone activity of the mouse ERG signal arises from the predominance of rods in the mouse retina, the rods constituting about 97% of the photoreceptors in mice (Carter-Dawson & LaVail, 1979). To avoid this complication, functionally rodless mice strains lacking different phototransduction proteins have been developed (Calvert et al., 2000; Humphries et al., 1997). However, these models allow the analysis of the cone-driven ERG of only young animals since the retinas of these transgenic animals appear to degenerate at young age.

As a very recent breakthrough, a brilliant method enabling a thorough characterization of the electrical properties of single mouse cones has been developed by Nikonov et al. (Nikonov, Kholodenko, Lem, & Pugh, 2006; Nikonov et al., 2005). In their method a set of photoreceptor inner segments is simultaneously sucked into a suction pipette. Then all the rod function is suppressed with a saturating background light, allowing the recording of cone photocurrents if one or more cone inner segments were present inside the pipette. The usage of the rod saturating background, however, brings about a complication, since the intense rod-suppressing illumination may affect the functional characteristics of the cone photoresponses.

* Corresponding author. Fax: +358 9 4513182.
E-mail address: hanna.heikkinen@hut.fi (H. Heikkinen).

0042-6989/$ - see front matter © 2007 Elsevier Ltd. All rights reserved.
doi:10.1016/j.visres.2007.11.005

The purpose of this work is to present the salient features of dark-adapted mouse cone photoresponses in the dark-adapted state, while avoiding the mechanical manipulation of the cells that is necessary in suction pipette method. We make use of the advantages of recording the aspartate-isolated electroretinogram from the isolated retina, i.e. the massed potentials reflecting the changes in the light sensitive current between the inner and outer segments. Instead of using strong rod saturating backgrounds we suppress the rod activity using preflashes intense enough to maintain rods in saturation, and then record cone flash responses we show to have recovered their dark-adapted state. Our approach combines the advantages of *in vivo* electroretinogram and single cell recordings: the cells remain intact in their virtually natural cellular environment, while they are still easily available for pharmalogical and environmental manipulations needed to ''purify'' the cone signals. Due to the extensive averaging across the recording area, the photoresponses are very repeatable, and the signal to noise ratio is good even though the cone ERG signals are small compared to rod signals. However, the analysis of the data recorded as mass potentials is complicated somewhat by the presence of two different pigments in mouse cones, one with absorption maximum at 360 nm and the other at 508 nm (Yokoyama & Yokoyama, 2000). The two pigments are coexpressed in different proportions in two subpopulations of cones, ''S-cones'' and ''M-cones'' (Jacobs, Neitz, & Deegan, 1991; Röchlich, van Veen, & Szél, 1994). In addition, there is a gradient in the expression ratio of these pigments within each population along the vertical direction of the retina (Applebury et al., 2000). Thus the distribution of the two pigments within the recording area may lead to different degrees of stimulation in individual cones, depending on the wavelength of stimulating light and each cone's S/M pigment ratio. However, stimulating selectively the M-pigment (thus giving rise to signal almost exclusively in ''M-dominated'' cones) we can arrive at a reasonable estimate of the average effective pigment density among the cones in the recording area and thus gain an estimate for the amount of pigment molecules activated by our stimuli.

The current work presents the basic characterisation of the mouse M-cone flash responses with respect to their sensitivity, kinetics and recovery from preceding rod-saturating stimuli. It portrays monophasic responses that are significantly faster than rod photoresponses and far less sensitive, while still surprisingly efficient in their activation phase, with an activation efficacy almost comparable to that of the rods.

2. Methods

2.1. Preparation, recording and light stimulation

2.1.1. The ERG experiments

Pigmented mice (C57Bl/6) were dark-adapted overnight or at least for 3 h (there was no difference apparent in the presented results between these protocols). The use and handling of all the animals in this study were in accordance with the Finland Animal Welfare Act 1986 with guidelines of the Animal Experimentation Committee of The University of Helsinki. The animals were sacrificed, the eyes were enucleated and bisected along the equator, and the retinas were detached in cooled Ringer under dim red light. The isolated retina was placed in a specimen holder (Donner, Hemilä, & Koskelainen, 1988) with an active recording area of 1.2 mm (diam.) at the flat-mounted central retina. The upper (photoreceptor) side was superfused with a constant flow (ca. 1.4 ml/min) of Ringer's solution containing (mM): Na^+ 133.9, K^+ 3.3, Mg^{2+} 2.0, Ca^{2+} 1.0; Cl^- 143.2, glucose, 10.0; EDTA, 0.01; Hepes, 12.0, buffered to pH 7.5–7.7 (at room temperature) with 5.8 mM NaOH. Leibovitz culture medium L-15 (Sigma), 0.72 mg/ml, was added to improve the viability of the retina. Sodium-L-aspartate (2 or 4 mM) was added to block synaptic transmission to second-order neurons. In addition, $BaCl_2$ (10 mM) was added in the lower electrode space, from where it would diffuse to the retina to suppress glial currents by blocking potassium channels located mainly at the endfeet of Müller cells (Bolnick, Walter, & Sillman, 1979; Nymark, Heikkinen, Haldin, Donner, & Koskelainen, 2005). The temperature (37 °C at the retina) was controlled by a heat exchanger below the specimen holder and monitored with a thermistor in the bath close to the retina (Ala-Laurila, Saarinen, Albert, Koskelainen, & Donner, 2002).

2.1.2. Recording and light stimulation

The transretinal potential was recorded with two Ag/AgCl pellet electrodes, one in the subretinal space and the other in chloride solution connected to the perfusion Ringer through a porous plug. The DC-signal was amplified 10,000×, filtered (2-pole) with low-pass frequency of 300 Hz, digitised commonly at 1000 Hz and stored on a computer hard disk for further analysis.

The flashes used to produce short flash stimuli with homogeneous full-field illumination to the distal side of the retina were provided by a dual-beam optical system adapted from the setup used by Donner et al. (1988). In brief, 16–20 ms light pulses were generated with a 543.5 nm HeNe laser (Melles Griot 05 LGR 173, 0.8 mW) and a Compur shutter, the midpoint of the flash indicating the zero-time for the recordings. The Gaussian profile of the laser beam was flattened by conducting the beam through a light guide with mixing fibers. The uniformity of the beam at the level of the retina was confirmed with a small aperture photodiode. To provide shorter stimuli specifically for cones, ca. 1.4 ms light pulses were generated from a computer controlled xenon flash gun (Minolta 360PX), with a broad spectrum of wavelengths selected using a long-pass edge filter (GG495 by Schott, $\lambda > 495$ nm). In some experiments the flash device was set to deliver ca. 10 ms pulses to achieve maximal stimulus. The light intensity of each source was controlled separately with calibrated neutral density filters and wedges.

2.2. Calibration of light intensities in terms of isomerised photopigments (Rh*) in rods and cones

The absolute intensity of the unattenuated laser beam (photons mm^{-2} s^{-1} incident on the retina) was measured in each experiment with a calibrated photodiode (EG&G HUV-1000B; calibration by the National Standards Laboratory of Finland). The intensity of the stimuli from the flash device was calibrated biologically with respect to the measured laser beam intensity by recording rod and cone responses to different stimuli from both devices and finding the relation in neutral density attenuation between devices that produced equivalent responses.

2.2.1. Conversion of stimulus intensity to Rh* in rods

To produce sensitivity and amplification parameters that are comparable between species and recording configurations, it is useful to express them in relation to the amount of isomerisations (Rh*) produced by the stimulating flash light in individual cells. In case of rods this is rather straightforward, and the end-on collecting area a_c of the rod can be calculated as (Baylor, Nunn, & Schnapf, 1984)

$$a_c = f\frac{\pi d^2}{4}[1 - 10^{-\Delta D(\lambda)l}]\gamma, \quad (1)$$

in which d and l are the diameter and length of the outer segments, respectively, $f \geqslant 1$ is a dimensionless factor that accounts for light funnelling by the inner segment and γ is the quantum efficiency of photoisomerization. $\Delta D(\lambda)$ is the specific density of the outer segment at wavelength λ. In our recording geometry the light enters the retina from the photoreceptor side, and thus the funnelling effect by the rod inner segments is negligible, i.e. $f = 1$. For the specific density of the outer segments at the wavelength of maximal absorption λ_{max} we adopt the value $\Delta D(\lambda_{max}) = 0.016$ o.d.units μm^{-1} (determined for rats rods by Nymark et al., 2005). Using the additional parameter values $d = 1.4$ μm, $l = 24$ μm (Carter-Dawson & LaVail, 1979) and $\gamma = 2/3$ we arrive at $a_{c,rod}(\lambda_{max}) = 0.73\ \mu m^2$. From the pigment template by Govardovskii, Fyhrquist, Reuter, Kuzmin, & Donner, 2000) we get $\Delta D(543.5\ nm) = 0.503\ \Delta D(\lambda_{max})$ for the mouse rods ($\lambda_{max} = 498$ nm, Lyubarsky et al., 1999), and we arrive at $a_{c,rod}(543.5\ nm) = 0.37\ \mu m^2$ for our stimulus wavelength. The number of isomerised pigment molecules Φ then relates to the stimulus intensity I_{hv} (as $h\nu\ \mu m^{-2}$) at given wavelength by

$$\Phi = I_{hv} \cdot a_c \tag{2}$$

2.2.2. Estimating number of isomerised pigments in cones

The estimation of photoisomerisation rates in cones is less straightforward, due to the varying percentage of M-opsin expressed in different cones and possible shadowing of cones by rod outer segments. We first estimate $a_{c,cone}$ in our ERG recording geometry assuming no shadowing by rods and 100% expression of M-pigment and thus the same optical density at absorption maximum as used for rods at their respective λ_{max}. The mouse cones taper very slightly into conical shape (Carter-Dawson & LaVail, 1979) and can be approximated as cylinders with a diameter of 1.2 μm and length 13.4 μm (Nikonov et al., 2006). Thus Eq. (1) yields $a_{c,cone}(\lambda_{max}) = 0.29\ \mu m^2$, representing the situation in which there is no pigment coexpression but all cones are exclusively S- or M-cones, out of which we stimulate only the M-cones measurably. We then take our estimation further by compensating the reduction of photon catch in our wavelength regime due to coexpression of pigments and shadowing by rods with corrective terms to produce an expression for the effective collection area of the M-cones in our recording geometry.

The rods of the flat-mounted retina in our recording geometry can be estimated to shadow the cones by approximately half of the length of their outer segments (cf. Fig. 6 of Carter-Dawson & LaVail, 1979). This will lead to a corrective term $k_{shadow} = 10^{-D(\lambda)*½}\ l_{rod} = 0.80$ to the 543.5 nm light reaching the cone outer segments, in which l_{rod} is the length of rod outer segment. It should be noted that this term is strongly wavelength dependent, becoming increasingly significant with wavelengths closer to the rod absorption maximum at which it reaches the minimum value of 0.64.

The second modification in the collection area must account for the distribution of S- and M-pigment in the cones of the central retina. It appears that the cones are divided into two main populations of "S-dominated" and "M/S"-cones with both the relative presentation of each population and the pigment expression levels within individual populations varying across the retina (Applebury et al., 2000; Nikonov et al., 2006). For a rigorous treatment of the problem, we would need to consider both of these varying factors, as even the "S-dominated" cones of the central retina respond noticeably to 500 nm light and thus must contain a significant fraction of M-pigment (Dr. Sergei Nikonov, personal communication). Lacking data of the exact fraction of cells in each population and the relative pigment distributions within populations, however, we will content with estimating the overall relative M-pigment level at the region of interest. From the data of Applebury et al. (2000, their Fig. 7.) we estimate that most cones in the central region of the retina contain S-pigment, the level of which remains rather constant in the nasal-temporal direction. The average percentage of M-pigment in the cells of this area is taken to be ca. 35%, out of total opsin concentration that is considered to remain practically constant. If S-pigment is deemed unresponsive to our stimuli, this percentage of "available opsin" will affect ΔD linearly: $\Delta D_{mod}(\lambda) = 0.35\ \Delta D(\lambda)$. This will lead into a corrective term of ca. 0.4 in our $a_{c,cone}$. Multiplying the stimulus intensity by k_{shadow} and replacing $\Delta D(\lambda)$ by $\Delta D_{mod}(\lambda)$ in Eq. (1), we get an estimation for the conversion factor from photon flux to isomerisation rate in the cones of the central retina: $k_{shadow}\ a_{c,cone,"M"} = 0.078\ \mu m^2$ at their λ_{max} and $0.067\ \mu m^2$ at 543.5 nm. Due to uncertainties in estimating the effective collecting areas, all the flash intensities in this work are primarily expressed in units of photons per μm^2 ($h\nu_\lambda\ \mu m^{-2}$) and both the sensitivity and amplification parameters of the cones are given with respect to these units as well as with respect to the estimated number of isomerisations per cell (Rh*). For comparability of values between experimental setups and cell types, also these "raw" intensities reported in subsequent text have been scaled to correspond to intensities at the λ_{max} of the specific cell type in question.

2.3. Analysis

The fractional amplitude vs. intensity data of cones were fitted with the Michaelis function

$$\frac{r(t_p)}{r_{sat}} = \frac{I_F}{I_F + I_{F,1/2}} \tag{3}$$

in which $r(t_p)$ is the response amplitude at the time of the peak (t_p) and r_{sat} is the amplitude of the saturated response. I_F is the flash intensity (either as photons, $h\nu_\lambda\ \mu m^{-2}$, or number of isomerised pigments per cell, Rh*) and $I_{F,½}$ is the half-saturating flash intensity. Fractional flash sensitivity S_F, i.e. the fraction of the photosensitive current turned off by unit flash intensity is related to the half-saturating flash intensity by $S_F = 1/I_{F,½}$. If the flash intensity is expressed as Rh*, S_F denotes the single photon response of the cell.

The respective rod data was fitted with an exponential that has previously (e.g. Nymark et al., 2005) been shown to fit well mammalian rod amplitude vs. intensity data at body temperature, i.e.

$$\frac{r(t_p)}{r_{sat}} = 1 - e^{-S_F \cdot I_F}. \tag{4}$$

With murine rod responses the determination of r_{sat} is somewhat controversial due to the "nose" component, a fast negative peak in the saturated photoresponses (see Fig. 1 and discussion there). The "nose" appears to be a transient component added to the saturated response, but it could also

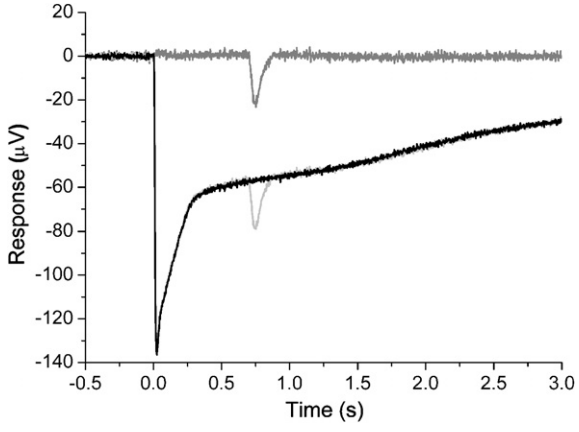

Fig. 1. Isolation of the cone photoresponses. The dark grey trace presents a massed photoresponse of cones to a test flash (xenon flash gun) corresponding to 8500 $h\nu_{508nm}\ \mu m^{-2}$. To obtain the isolated cone response, the following two different responses were recorded: the black trace represents a response to a rod-saturating flash ("preflash only", a 20 ms flash delivering 170,000 $h\nu_{508nm}\ \mu m^{-2}$) and the light grey trace represents a response to a preflash, followed by the test flash at 700 ms ("double flash"). The pure cone response to the test flash is obtained by subtracting the response to the preflash only from the response to the double flash. Each response is averaged from 2–3 trials.

be a longer-lasting component of opposite polarity. As there is not yet conclusive evidence supporting either of these hypotheses, and because the plateau level of saturated responses appears not to be affected by e.g. background light while the peak level of the nose is strongly affected, we chose the plateau level to reflect rod saturation amplitude. In case of the nose peak truly reflecting the saturation amplitude instead, r_{sat} would be up to 40% larger.

To quantify the activation kinetics of the responses, the activation phase of the normalized responses was fitted with a phototransduction model by Lamb and Pugh (1992),

$$\frac{r(t)}{r_{sat}} = 1 - \exp[-\frac{1}{2}\Phi A(t - t_d)^2], \quad (5)$$

in which $r(t)$ is the response waveform and r_{sat} is the saturated response amplitude. Φ is the stimulus intensity in photoisomerisations per cell and A is an activation coefficient (in sec^{-2}). The delay parameter t_d combines several small delays in the activation cascade.

For cones, the activation model (Eq. (5)) was convolved with an exponential delay presenting the cell's membrane time constant τ (which e.g. in human cones is about 5 ms, Smith & Lamb, 1997). The time constant is significantly smaller in rods compared to cones, and due to the slower kinetics of rod photoresponses, the effect of time constant on the waveform is negligible in rods, and the time constant may be lumped into the overall delay, t_d.

The inactivation kinetics of both rods and cones were quantified with determination of the dominant time constant τ_{rec} of the response inactivation (the "Pepperberg" analysis, introduced by Pepperberg et al., 1992) from the time required for 20% recovery of the responses to saturating flashes.

3. Results

3.1. Isolation of the M-cone responses

Aspartate-isolated photoresponses of the mouse retina contain components from both rod and cone origin. The cone component in our recordings can be considered to be driven solely by activation of M-pigment: even at the shortest stimulating wavelengths used in this work, the absorbance of S-pigment has already diminished to less than 1/500,000 of its maximum (based on pigment templates by Govardovskii et al., 2000), while the peak sensitivities of S- and M-pigment dominated cones appear to be essentially similar (Nikonov et al., 2006). On the other hand, the M-cone photoresponses cannot be distinguished from the rod responses by spectral means due to the similarity of their spectral sensitivity characteristics, but the differences in kinetics and sensitivity of these two cell types enable isolation of pure cone responses (Fig. 1). The black trace in Fig. 1 illustrates a typical response to a strong, rod saturating flash (intensity I_{PF}). The initial phase of the response comprises of a mixture of a cone response, a relatively slowly activating rod response and a rapidly decaying negative component, a "nose". After *ca.* 300 ms, the initial transient part of the response containing both the "nose" and the cone response has returned to the baseline, and all that remains is the saturated rod response. The light grey trace that mostly overlaps the black one represents responses to a pair of subsequent flashes: a rod-saturating preflash (intensity I_{PF}) followed by a test flash (I_F), the response that originates only in cones due to the maintained saturation of rods. The dark grey trace in Fig. 1 is the pure cone response that results from subtracting the response to "preflash only" from the response to "preflash followed by the test flash".

The initial "nose" is especially prominent in the retina of Fig. 1, adding generally up to 40% to the amplitude determined at the saturated plateau of our mouse rod records (when cone equivalent component removed; not shown in the figure). It is mainly originated in rods, and is likely generated at least in part by currents through the voltage sensitive channels in the inner segments of these cells (Bader, MacLeish, & Schwartz, 1979; Barnes & Hille, 1989; Fain, Quandt, Bastian, & Gerschenfeld, 1978; Green & Kapousta-Bruneau, 1999). No corresponding component will be generated in response to a test flash while the rods remain saturated. Thus while the "nose" affects the analysis of the waveform and amplitude of the saturated rod responses, no effect due to it can be observed in our test flash (cone) responses.

3.2. Recovery of the cone response after a rod-saturating preflash

The rod-saturating preflash preceding the test flash in Fig. 1 is intense enough to stimulate cones to a considerable extent. To examine pure cone photoresponses in a dark-adapted state, it is vital for the cones to have fully recovered from their response to the preflash at the time of the test flash. To ensure this, we examined the recovery of the cone responses to an approximately half-saturating test flash (intensity I_F) as a function of the interval (Δt_{flash}) between consecutive flashes. Fig. 2 presents a set of cone

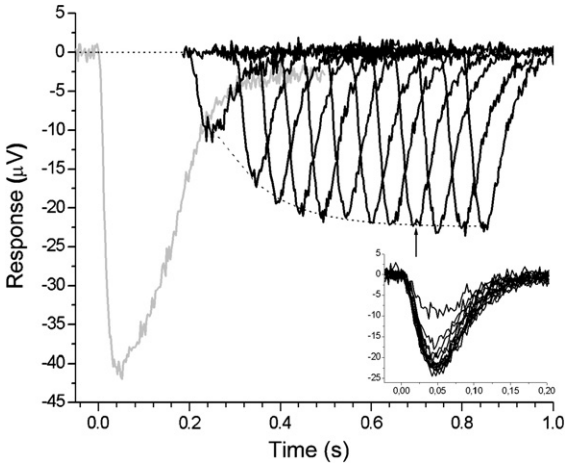

Fig. 2. Recovery of the cone response after the preflash. The grey trace represents an isolated cone response to a test flash equivalent to the rod-saturating preflash (xenon flash gun, $I = 170{,}000$ hv_{508nm} μm^{-2}), given at time $t = 0$. The black traces represent the cone responses to the test flash (xenon flash gun, $I = 8500$ hv_{508nm} μm^{-2}) at different times Δt_{flash} after the preflash. The data is from the same retina as in Figs. 1 and 3, each response presents an average from 2–3 trials. The response designated with an arrow ($\Delta t_{flash} = 700$ ms) is produced with the flash interval used throughout the rest of the experiment. The dotted curve fitted to the response peaks describes the recovery of the response amplitude as a product of five exponentials ($\tau = 105$ ms) and the straight dashed line denotes the recovered response amplitude of 22.4 μV. The inset presents the cone responses to the test flash shifted on the time scale to begin at $t = 0$.

photoresponses from the same retina as in Fig. 1 to $I_F = 8500\ h\nu_{508nm}\ \mu m^{-2}$ with Δt_{flash} varying from 200 to 800 ms. The light grey response at time $\Delta t_{flash} = 0$ is the cone response to a test stimulus photopically equal to the preflash ($I_F = 170\ 000\ h\nu_{508nm}\ \mu m^{-2}$). The arrow marks the preflash—test flash interval ($\Delta t_{flash} = 700$ ms) used during the rest of the experiment.

While the cone response to the preflash temporarily diminishes the amplitude of the cells' responses to subsequent stimuli, it is noteworthy that it does not change the response kinetics. The responses are simply scaled down due to the adapting effect of the previous response, but not visibly accelerated or decelerated (see inset in Fig. 2). The recovery of the diminished response amplitude is swift, once Δt_{flash} exceeds the time at which the cone response to the preflash has returned to the baseline, the isolated cone response to I_F has fully recovered its amplitude. The response amplitude as a function of time after the preflash was well fitted with a product of five decaying exponentials (the dotted curve in the figure, $r = r_o\ (1 - \exp(-t/\tau))^5$, $r_o = 22.2\ \mu V$, $\tau = 105$ ms).

With the preflash stimuli used in this study (I_{PF} within $1.1 \times 10^5 - 2.2 \times 10^6\ h\nu_{508nm}\ \mu m^{-2}$) the time intervals needed for recovery periods were ca. 500–1000 ms, thus setting the lower limit for Δt_{flash} in each experiment. An upper limit to the range of valid flash intervals, ca. 1000–1500 ms was set by the rod saturation time, which also had to be estimated separately for each retina as extending Δt_{flash} beyond the rod saturation would have led to impure cone responses with a rod component superimposed.

3.3. Waveform, sensitivity and kinetics of the cone responses

3.3.1. The general characteristics of the responses

Fig. 3a presents a family of cone photoresponses from the same retina as in Figs. 1 and 2, portraying the typical qualitative features of our cone recordings. As opposed to the photoresponses from isolated cones of human (Kraft, Neitz, & Neitz, 1998) and macaque (Schnapf, Nunn, Meister, & Baylor, 1990) but resembling the ERG data from human (Friedburg, Allen, Mason, & Lamb, 2004) and suction pipette recordings from mouse (Nikonov

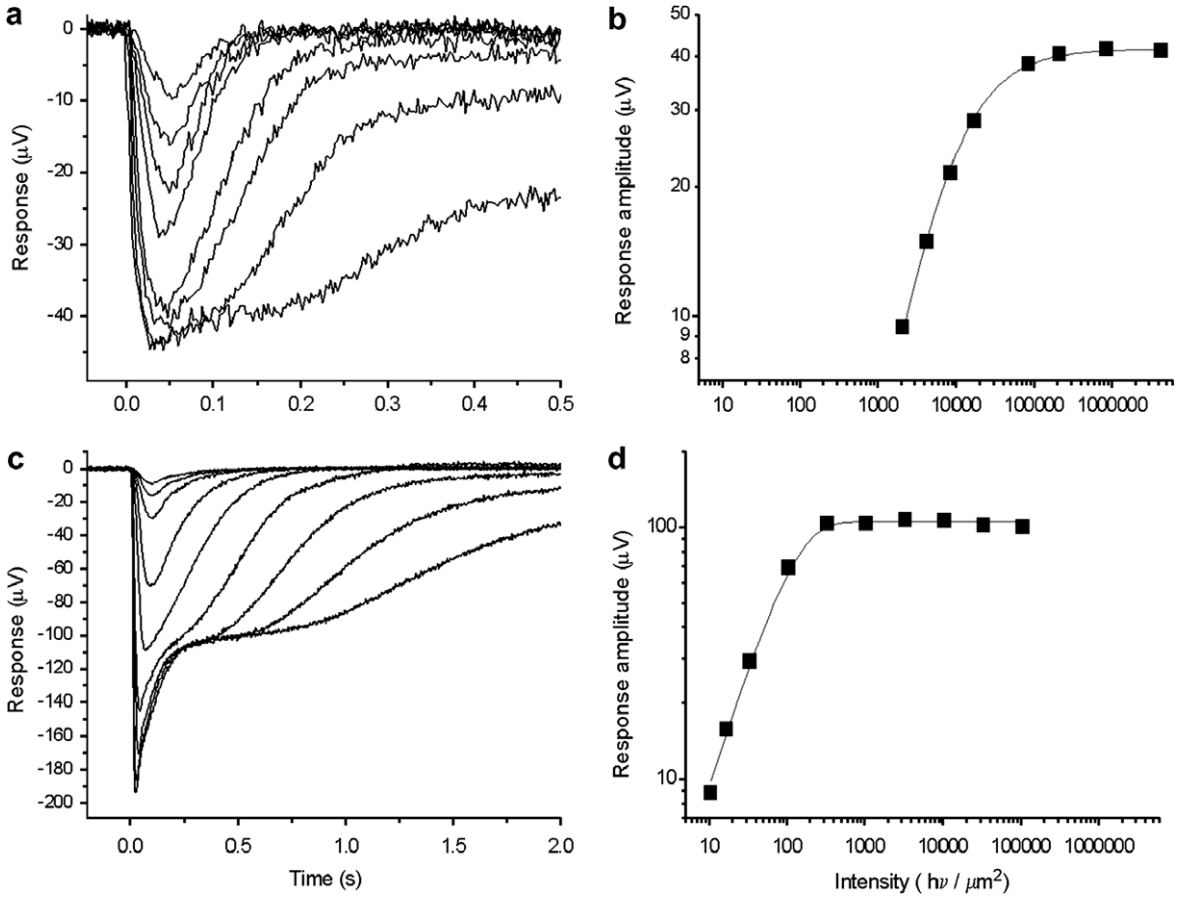

Fig. 3. (a) A family of cone photoresponses from the same retina as in Figs 1 and 2 to a set of stimuli generated with the xenon flash gun, yielding 2100, 4300, 8500, 17,000, 85,000, 210,000, 850,000 and 4300,000 $h\nu_{508nm}\ \mu m^{-2}$. (b) The amplitude-intensity curve from the responses in (a). The data was fitted with a Michaelis function (Eq. (3)), giving parameters $U_{sat} = 42\ \mu V$ and $I_{½} = 7500\ h\nu_{508nm}\ \mu m^{-2}$, corresponding to single photon response of $S_F = 0.0017\ (Rh^*)^{-1}$. (c) The rod photoresponses (with a cone component superimposed to the largest responses) from the same retina to 20 ms flashes yielding yielded 10, 16, 31, 100, 310, 1000, 3100, 10,000, 31,000 and 100,000 $h\nu_{498nm}\ \mu m^{-2}$ and (d) the amplitude-intensity curve for the responses in (c). Fitting this data with Eq. (4), resulted in parameters $U_{sat} = 105\ \mu V$ and $S_F = 0.009\ (h\nu_{498nm}\ \mu m^{-2})^{-1}$, corresponding to ca. $0.013\ (Rh^*)^{-1}$.

et al., 2006) as well as ground squirrel (Kraft, 1988), the responses are overall monophasic. The saturated responses contain a small, fast negative "nose", followed by extended plateau of saturation, resembling the behavior of rod responses in both respects (Fig. 3c). The cone "nose" component was visible in 6 out of 7 retinas. The small-stimulus responses (amplitude 22% of the saturated response) peak at 55 ms in this retina (the range of t_p determined from responses reaching 15–25% of the saturated amplitude in 9 retinas was 43–58 ms, with a mean of 51 ± 2 ms, SEM). Thus the cones were over two-fold faster than the rods from the same set of retinas ($t_p = 117 \pm 3$ ms). The cone amplitude-intensity data was well fitted with a Michaelis-curve (Eq. (3)) with half-saturating stimulus intensity $I_{½} = 7500$ $h\nu_{508nm}$ μm^{-2}, corresponding to $\Phi =$ 580 Rh^* and a single-photon response S_F of 0.17% per Rh^*. The $I_{½}$ values from 9 retinas ranged from 2500 to 8500 $h\nu_{508nm}$ μm^{-2}, with a mean of 5500 ± 700 $h\nu_{508nm}$ μm^{-2}, corresponding to $\Phi_{½} = 430 \pm 50$ Rh^* and $S_F = 0.23\%$. The respective rod data from the same retina followed closely an exponential relation (Eq. (4)) with $S_F = 1.3\%$ per Rh^* in each rod (average $1.2 \pm 0.3\%$ per Rh^*; $n = 10$).

3.3.2. The amplification and recovery kinetics

To further quantify the kinetics of the cones, the Lamb and Pugh activation model (Eq. (5)) was fitted to the rising edge of the responses. Fig. 4a and b illustrate results of one such fit, with the rod responses from the same retina presented for comparison in Fig. 4c and d. To achieve qualitatively best fit, it proved vital to normalise the responses of both cell types according to the saturation level following the "nose" part of the responses, instead of just using the maximal response amplitude (cf. Nikonov et al., 2006; Nymark et al., 2005). Then only rising phase of the subsaturated responses were used in the fitting. The rod responses were well fitted with Eq. (5), without a noticeable improvement to the fit when filtering due to a membrane time constant was introduced to the model. However, the membrane time constants used in fitting the theoretical

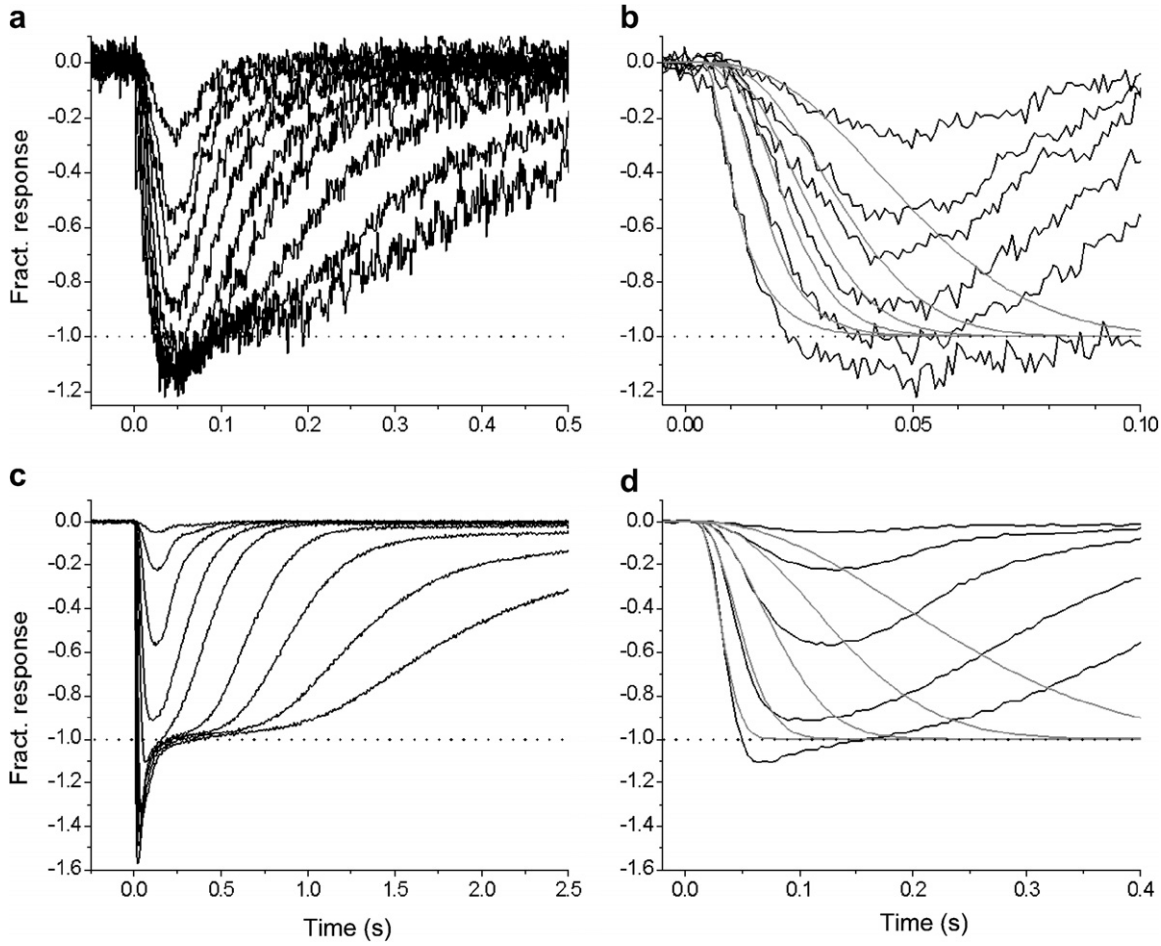

Fig. 4. (a) A family of cone photoresponses with the saturation "plateau" denoted with dotted line in response to flashes of $I = 2400$, 5900, 12,000, 24,000, 59,000, 120,000, 240,000, 590,000, 1200,000 and 2400,000 $h\nu_{508nm}$ μm^{-2}. (b) The 5 smallest and the largest response from (a) fitted with the Lamb and Pugh activation model (Eq. (5)). (c) The rod photoresponses from the same retina to intensities of $I = 4.3$, 14, 43, 140, 430, 1400, 4300, 14,000 and 43,000 $h\nu_{498nm}$ μm^{-2}, with a cone component superimposed to the largest responses. (d) The responses to 5 smallest stimuli from (c) fitted with the Lamb and Pugh activation model. The model parameters for cones are: $A = 5.4$ s^{-2}, $\tau_m = 7$ ms and $t_d = 5$ ms, and for rods: $A = 6.7$ s^{-2}, τ_m=1 ms and $t_d = 11$ ms.

curves to the cone data were slightly higher than found in literature (mean 6.5 ± 0.3 ms; $n = 6$), possibly reflecting other damping factors in our experimental conditions, such as the differences of M-pigment concentration and/or differences in the photoresponse kinetics between individual cones. The mean amplification coefficient A_{cone} for cones was 0.36 ± 0.03 s $^{-2}/a_c$, in which a_c is the conversion factor from the flash intensity in hν μm^{-2} at λ_{max} to photoisomerisations. Using the effective collecting area derived in Section 2, this leads to an estimate of $A_{cone} = 4.6 \pm 0.4$ s^{-2}. The rod amplification coefficient was only slightly higher to the estimates for cones, with a mean of $A_{rod} = 5.6 \pm 0.7$ s $^{-2}$. This difference in the amplification coefficient can be taken as an overestimate, since the difference may be removed if we reconsider our assumption of the normalization level of saturated photoresponses. While the "nose" adds up to 40% to the saturated amplitude in rods (effectively lowering the amplification coefficient by about same factor), its effect in cones is significantly smaller, ranging from 0 to 15% in the retinas of the present study. If the nose truly reflected the photoresponse proper, i.e the changes in the light-sensitive current, the corrections in photoresponse saturation amplitude would lead to an amplification constant of ca. 4.0 for both rods and cones.

The kinetics of the response inactivation phase can be characterized with a single parameter, the dominant time constant of recovery τ_{rec} (Pepperberg et al., 1992). By linear fit to the time for recovery of 20% from the saturation level vs. the natural logarithm of stimulus intensity (see Fig. 5) we found $\tau_{rec} = 33 \pm 4$ ms ($n = 3$) for cones compared to $\tau_{rec} = 160 \pm 7$ ms for the rods in the same retinas.

4. Discussion

Isolated retina presents a model for phototransduction studies, in which the photoreceptor cells remain intact and maintain their natural retinal surroundings. While they need not be mechanically manipulated to obtain photoresponse recordings, they are still readily available for pharmacological treatments and environmental changes, e.g. regarding temperature, pH, etc. In the present study we have described the basic functional parameters of dark-adapted photoresponses from mouse M-cones, providing a bridge between electroretinogram studies of living animals and single cell suction pipette recordings. The ERG of live subjects is non-invasive to the retinal cells but pure photoreceptor light responses are tedious to obtain due to intervening signal components, while suction pipette recordings are a straight-forward way to study photoreceptor function but rather mechanically distressing to the cells under investigation. It is thus interesting to make comparisons of the photoreceptor response parameters from the isolated retina to those obtained by the above-mentioned techniques.

Cone photoresponses are generally characterized as fast and relatively insensitive, with 3–4 times smaller time-to-peak (t_p) values and 10- to 35-fold lower flash sensitivity than in rods of each species (for a review, see e.g. Pugh & Lamb, 2000). The dark-adapted mouse cone responses currently described are noticeably slower than reported for some mammals, such as ground squirrel (Kraft, 1988, ca. 20 ms) and human (Friedburg et al., 2004, 15–20 ms). With t_p of ca. 50 ms (range 43–63 ms), our cone responses

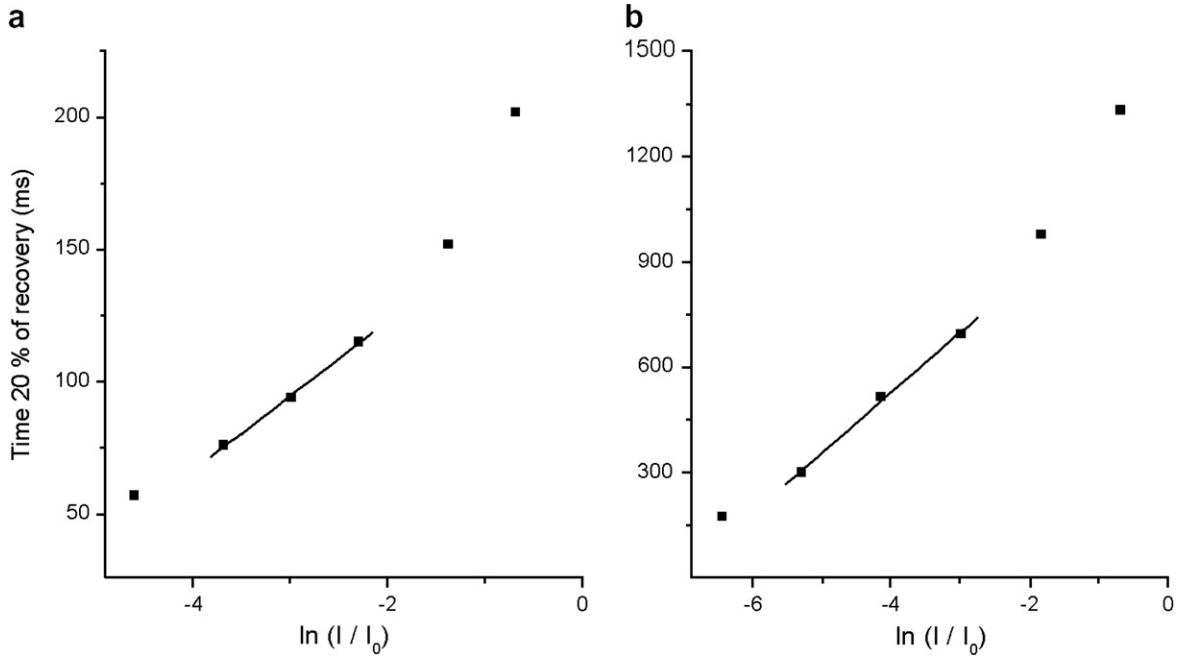

Fig. 5. Deactivation kinetics of (a) cones and (b) rods quantified with a Pepperberg-plot. τ_{rec}, the dominant time constant of deactivation was 28 ms for the cones and 171 ms for the rods in this retina. The intensities used to produce the cone responses in (a) were 24,000, 59,000, 120,000, 240,000 and 590,000 and 1200,000 hν$_{508nm}$ μm^{-2} and 140, 430, 1400, 4300, 14,000 and 43,000 hν$_{498nm}$ μm^{-2} for the rod responses (b).

show very similar if slightly larger t_p values to the 60–70 ms obtained for mouse by Nikonov et al. (2006) in their suction pipette recordings (taking into account the 22 ms delay in their recordings due to the analog filtering; Dr. Nikonov, personal communication), implying this to be characteristic kinetic behavior for the dark-adapted mouse cones.

Due to differences in geometrical configurations, any comparisons of the sensitivity parameters obtained with various experimental techniques must be based on estimates of Rh* caused by the stimuli in each case. When expressed in terms of photoisomerizations, our rod to cone sensitivity ratio is surprisingly small, rod single photon response being only ca. 5-fold bigger than that of the cones. Due to differences in the respective collecting areas, the ratio is significantly larger, about 40 when stimuli are expressed as intensities (at the respective λ_{max} of cones and rods). The fractional sensitivity values of ca. 0.2% per Rh* are very similar when determined with the two available recording methods for wild type cones (current work and Nikonov et al., 2006). The rod flash sensitivities obtained by these two methods, however, differ ca. 3- to 5-fold, with a single photon response of 1.2% by our ERG compared to the substantially higher values obtained with suction pipette method by Nikonov et al. (2006) and Krispel et al. (2006). The rod sensitivity value reported here may be close to the values obtainable *in vivo*, instead. Kang Derwent et al. (2007) have reported sensitivity parameter of 4.79 (sc cd s m^{-2})$^{-1}$, which corresponds to S_F of ca. 1–2% per Rh* when using the intensity conversion factors determined by Lyubarsky, Daniele, and Pugh (2004). The differences in rod sensitivity between ERG and suction pipette can be largely explained by the slower shut down kinetics in suction pipette recordings. While the quite similar activation coefficients of the rod photoresponses determined with either ERG *in vivo* (6.2 s^{-2}, Lyubarsky et al., 2004), our ERG on isolated retinas (5.6 s^{-2}) or suction pipette (7.6 – 8.4 s^{-2}, Nikonov et al., 2005) are too close to each other to explain the differences in the flash sensitivities, there seem to be considerable differences in time to peak-values and recovery time constants between the techniques, specifically between ERG and single cell recordings. The mouse rod photoresponses determined in ERG (*in vivo* or isolated retina) peak close to 100 ms (ca. 93 ms by Hetling & Pepperberg, 1999; 117 ms in current work, our parameter being affected somewhat due to the 20 ms flash stimulus beginning at $t = -10$ ms), while there is much more variation in the time to peak values recorded with single cell recordings (e.g. 126 ms by Krispel et al., 2006; 180–190 ms by Nikonov et al., 2005, taking into account the delay by analog filtering). Similar differences in t_p-values between ERG and suction pipette methods can be found for monkey and human (cf. Friedburg, Thomas, & Lamb, 2001, their Table 1). Also time constants of recovery reported for mouse rods in the same studies are longer when determined by single cell recordings.

The origins of the low sensitivity of the cones compared to that of the rods deserve a bit of further inspection. It seems intuitive and straightforward to associate low sensitivity with low gain in phototransduction, along with the faster shut down kinetics of the photoresponse. Low amplification rate of cones has been determined for fish (Tachibanaki, Tsushima, & Kawamura, 2001), but is not necessarily the case in mammals. Our data indicates very similar efficacies of activation in rods and cones, and is in line with the work by Smith and Lamb (1997), who found comparable estimates for amplification coefficients of human rods and cones. Although there is slightly larger, twofold difference in the rod/cone activation coefficient ratio determined by Nikonov et al. (2006), it is yet too small to explain the difference between rod and cone single photon responses. Thus given the relatively high gain in the activation of the mouse cone photoresponse, the low cone sensitivity must be attributed almost entirely to faster inactivation kinetics of the cone flash response compared to rods, which is in line with the faster dominant time constant of recovery in cones.

Acknowledgments

We are grateful for Dr. Kristian Donner, Dr. Simo Hemilä and Dr. Sergei Nikonov for their insightful comments on the manuscript. We also thank Mr. Petri Kärkäs for his assistance with some of the experiments. This work was supported by the Academy of Finland and the Finnish Cultural Foundation.

References

Ala-Laurila, P., Saarinen, P., Albert, R., Koskelainen, A., & Donner, K. (2002). Temperature effects on spectral properties of red and green rods in toad retina. *Visual Neuroscience, 19*, 785–792.

Applebury, M. L., Antoch, M. P., Baxter, L. C., Chun, L. L. Y., Falk, J. D., Farhangfar, F., Kage, K., Krzystolik, M. G., Lyass, L. A., & Robbins, J. T. (2000). The murine cone photoreceptor: A single cone type expresses both S and M opsins with retinal spatial patterning. *Neuron, 27*, 513–523.

Bader, C. R., MacLeish, P. R., & Schwartz, E. A. (1979). A voltage-clamp study of the light response in solitary rods of the tiger salamander. *Journal of Physiology, 296*, 1–16.

Barnes, S., & Hille, B. (1989). Ionic channels of the inner segment of tiger salamander cone photoreceptors. *Journal of General Physiology, 94*, 719–743.

Baylor, D. A., Nunn, B. J., & Schnapf, J. L. (1984). The photocurrent, noise and spectral sensitivity of rods of the monkey Macaca fascicularis. *Journal of Physiology, 357*, 575–607.

Bolnick, D. A., Walter, A. E., & Sillman, A. J. (1979). Barium suppresses slow PIII in perfused bullfrog retina. *Vision Research, 19*, 1117–1119.

Calvert, P. D., Krasnoperova, N. V., Lyubarsky, A. L., Isayama, T., Nicolo, M., Kosaras, B., Wong, G., Gannon, K. S., Margolskee, R. F., Sidman, R. L., Pugh, E. N., Jr., Makino, C. L., & Lem, J. (2000). Phototransduction in transgenic mice after targeted deletion of the rod transducin alpha-subunit. *Proceedings of the National Academy of Sciences, 97*, 13913–13918.

Carter-Dawson, L. D., & LaVail, M. M. (1979). Rods and cones in the mouse retina. *Journal of Comparative Neurology, 188*, 245–262.

Donner, K., Hemilä, S., & Koskelainen, A. (1988). Temperature-dependence of rod photoresponses from the aspartate-treated retina of the frog (Rana temporaria). *Acta Physiologica Scandinavica, 134*, 535–541.

Fain, G. L., Quandt, F. N., Bastian, B. L., & Gerschenfeld, H. M. (1978). Contribution of a caesium-sensitive conductance increase to the rod photoresponse. *Nature, 272*, 466–469.

Friedburg, C., Thomas, M. M., & Lamb, T. D. (2001). Time course of the flash response of dark- and light-adapted human rod photoreceptors derived from the electroretinogram. *Journal of Physiology, 534*, 217–242.

Friedburg, C., Allen, C. P., Mason, P. J., & Lamb, T. D. (2004). Contribution of cone photoreceptor and post-receptoral mechanisms to the human photopic electroretinogram. *Journal of Physiology, 556*, 819–834.

Govardovskii, V. I., Fyhrquist, N., Reuter, T., Kuzmin, D. G., & Donner, K. (2000). In search of the visual pigment template. *Visual Neuroscience, 17*, 509–528.

Green, D. G., & Kapousta-Bruneau, N. V. (1999). A dissection of the electroretinogram from the isolated rat retina with microelectrodes and drugs. *Visual Neuroscience, 16*, 727–741.

Hetling, J. R., & Pepperberg, D. R. (1999). Sensitivity and kinetics of mouse rod flash responses determined in vivo from paired-flash electroretinograms. *Journal of Physiology, 516*, 293–609.

Hood, D. C., & Birch, D. G. (1990). A quantitative measure of the electrical activity of human photoreceptors using electroretinography. *Visual Neuroscience, 5*, 379–387.

Humphries, M. M., Rancourt, D., Farrar, G. J., Kenna, P., Hazel, M., Bush, R. A., Sieving, P. A., Sheils, D. M., McNally, N., Creighton, P., Erven, A., Boros, A., Gulya, K., Capecchi, M. R., & Humphries, P. (1997). Retinopathy induced in mice by targeted disruption of the rhodopsin gene. *Nature Genetics, 15*, 216–219.

Jacobs, G. H., Neitz, J., & Deegan, J. F. II, (1991). Retinal receptors in rodents maximally sensitive to ultraviolet light. *Nature, 353*, 655–656.

Jacobs, G. H., Williams, G. A., & Fenwick, J. A. (2004). Influence of cone pigment coexpression on spectral sensitivity and color vision in the mouse. *Vision Research, 44*, 1615–1622.

Kang Derwent, J. J., Saszik, S. M., Maeda, H., Little, D. M., Pardue, M. T., Frishman, L. J., & Pepperberg, D. R. (2007). Test of the paired-flash electroretinogram method in mice lacking b-waves. *Visual Neuroscience, 24*, 141–149.

Kraft, T. W. (1988). Photocurrents of cone photoreceptors of the gold-mantled ground squirrel. *Journal of Physiology, 404*, 199–203.

Kraft, T. W., Neitz, J., & Neitz, M. (1998). Spectra of human L cones. *Vision Research, 3*, 3663–3670.

Krispel, C. M., Chen, D., Melling, N., Chen, Y. J., Martemyanov, K. A., Quillinan, N., Arshavsky, V. Y., Wensel, T. G., Chen, C. K., & Burns, M. E. (2006). RGS expression rate-limits recovery of rod photoresponses. *Neuron, 51*, 409–416.

Lamb, T. D., & Pugh, E. N. Jr., (1992). A quantitative account of the activation steps involved in phototransduction in amphibian photoreceptors. *Journal of Physiology, 449*, 719–758.

Lyubarsky, A. L., Falsini, B., Pennesi, M. E., Valentini, P., & Pugh, E. N. Jr., (1999). UV- and midwave-sensitive cone-driven retinal responses of the mouse: A possible phenotype for coexpression of cone photopigments. *Journal of Neuroscience, 19*, 442–455.

Lyubarsky, A. L., Daniele, L. L., & Pugh, E. N. Jr., (2004). From candelas to photoisomerizations in the mouse eye by rhodopsin bleaching in situ and the light-rearing dependence of the major components of the mouse ERG. *Vision Research, 44*, 3235–3251.

Nikonov, S. S., Daniele, L. L., Zhu, X., Craft, C. M., Swaroop, A., & Pugh, E. N. Jr., (2005). Photoreceptors of Nrl−/− mice coexpress functional S- and M-cone opsins having distinct inactivation mechanisms. *Journal of General Physiology, 125*, 287–304.

Nikonov, S. S., Kholodenko, R., Lem, J., & Pugh, E. N. Jr., (2006). Physiological features of the S- and M-cone photoreceptors of wild-type mice from single-cell recordings. *Journal of General Physiology, 127*, 359–374.

Nymark, S., Heikkinen, H., Haldin, C., Donner, K., & Koskelainen, A. (2005). Light responses and light adaptation in rat retinal rods at different temperatures. *Journal of Physiology, 567*, 923–938.

Pepperberg, D. R., Cornwall, M. C., Kahlert, M., Hofmann, K. P., Jin, J., Jones, G. J., & Ripps, H. (1992). Light-dependent delay in the falling phase of the retinal rod photoresponse. *Visual Neuroscience, 8*, 9–18.

Pugh, E. N., Jr., & Lamb, T. D. (2000). Phototransduction in vertebrate rods and cones: Molecular mechanisms of amplification recovery and light adaptation. In D. G. Stavenga, W. J. de Grip, & E. N. Pugh, Jr. (Eds.). *Handbook of biological physics, Molecular mechanisms of visual transduction* (Vol. 3, pp. 183–255). Amsterdam: Elsevier.

Röchlich, P., van Veen, T., & Szél, Á. (1994). Two visual pigments in one retinal cone cell. *Neuron, 13*, 1166–1959.

Smith, N. P., & Lamb, T. D. (1997). The a-wave of the human electroretinogram recorded with a minimally invasive technique. *Vision Research, 37*, 2943–2952.

Schnapf, J. L., Nunn, B. J., Meister, M., & Baylor, D. A. (1990). Visual transduction in cones of the monkey Macaca fascicularis. *Journal of Physiology, 427*, 681–713.

Tachibanaki, S., Tsushima, S., & Kawamura, S. (2001). Low amplification and fast visual pigment phosphorylation as mechanisms characterizing cone photoresponses. *PNAS, 98*, 14044–14049.

Yokoyama, R., & Yokoyama, S. (2000). Comparative molecular biology of visual pigments. In D. G. Stavenga, W. J. de Grip, & E. N. Pugh, Jr. (Eds.), *Molecular mechanisms in visual transduction* (pp. 257–296). New York: Elsevier Science Publishing Co., Inc.